AN ABSTRACTED MODEL FOR ESTIMATING TEMPERATURE AND RELATIVE HUMIDITY IN THE POTENTIAL REPOSITORY AT YUCCA MOUNTAIN

Sitakanta Mohanty and George Adams

Center for Nuclear Waste Regulatory Analyses

Southwest Research Institute®, San Antonio, TX 78238

ABSTRACT

This paper presents an abstracted model for estimating relative humidity and temperatures in the potential high-level waste repository at Yucca Mountain, Nevada, USA. The abstracted model is one component in a larger probabilistic model that requires numerous Monte Carlo realizations to compute performance of the repository system [1]. The abstracted model estimates the repository-horizon rock temperature using a mountain-scale analytical heat conduction model with the waste emplacement drifts as the heat sources (adjusted for heat losses caused by ventilation) residing in a semi-infinite medium. Also included in the abstracted model is a simplified thermal network model, which uses drift-scale heat transfer through various engineered components and air gaps to estimate the waste package (WP) surface temperature from the rock temperature computed by the mountain-scale model. This drift-scale heat transfer is represented in terms of an equivalent conduction for various heat transfer models (i.e., conduction, convection, and radiation). Relative humidity is computed from a standard thermodynamic equation relating vapor pressure to temperature.

I. INTRODUCTION

One key aspect of assessing performance of the potential high-level waste (HLW) repository at Yucca Mountain, Nevada, USA, is to estimate the temperature of the engineered system and the surrounding medium for a given repository design. Heat is generated by the radioactive decay of spent nuclear fuel (SNF) disposed in WPs emplaced in drifts excavated in the rock nearly 350 m below the ground surface. Based on one scenario analysis, leading hypotheses on how temperature could influence various processes in the repository include the following:

- The heat will evaporate infiltrating water and create a dryout zone around the drifts. Above the repository horizon, the water vapor will condense and flow back toward the repository by gravity, thus creating a reflux zone even when the temperature is above boiling in the drift. Water entering the drift at high temperature may impinge on the drip shield surrounding the WPs and contribute to drip shield corrosion. Water flowing into the drift could change the humidity condition in the drift contributing to WP corrosion.
- Temperature can influence fluid chemistry through geochemical interaction between rock and fluids.
- Temperature can influence rock mechanics through thermal expansion of fractured rock mass.

- Higher temperatures could make WPs more vulnerable to failures because of the augmented chemical condition, even at low relative humidity (RH) [2].
- The waste form itself may be vulnerable to faster dissolution at high temperatures with the resulting aggressive chemical conditions [2].

Clearly, the processes through which heat can influence repository performance are coupled. A detailed simulation model that includes all the couplings among processes (e.g., thermal, hydrological, chemical, and mechanical) occurring at various length scales, heterogeneities in physical and chemical properties, and other complexities cannot be incorporated into the repository system level model and still maintain reasonable computer execution times in a probabilistic manner. Hence, there is a need for an abstracted model. The key to developing an abstracted model is to simplify the model by systematically decoupling the processes and incorporating the level of detail necessary to produce a credible analysis that provides meaningful insights into performance.

This paper presents the mathematical model for evaluation of the temperature and RH throughout the immediate space surrounding the potential repository for 10,000 years. Section II of this paper provides a brief description of the repository site and the repository environment. Section III presents the abstracted conceptual and mathematical models for estimating temperature at the mountain scale and the repository scale. Section IV provides a description of the system model. Section V presents assumptions. Section VI describes results from the deterministic and stochastic calculations. Section VII presents the conclusions.

II. DESCRIPTIONS OF PROPOSED SITE AND REPOSITORY

Yucca Mountain is 40 km long by 6–10 km wide. The stratigraphy at Yucca Mountain is composed of a gently dipping sequence of ash-flow tuffs, lavas, and volcanic breccias more than 1,800 m thick. The mountain is dominated by a subparallel series of ridges controlled by steeply dipping faults. The rock unit being considered for the potential repository facility is a densely welded ash-flow tuff of the Topopah Spring Member of the Paintbrush Tuff. The crest of the mountain varies between altitudes of 1,500 and 1,930 m or nearly 650 m higher than the floor of Crater Flat to the west of the site. The depth of the groundwater table

from the repository horizon is approximately 350 m directly below the repository block. Climate at the site is generally arid to semiarid, with an average precipitation of nearly 180 mm/yr.

The potential repository at Yucca Mountain is an underground facility designed to accommodate 70,000 metric tons of HLW. The waste disposed in the repository is expected to consist of both commercial SNF (~90 percent in terms of activity) and defense and other HLW (~10 percent in terms of activity), with an age of 5–50 years. The specific layout of the underground facility used for this study is based on the U.S. Department of Energy (DOE) new Enhanced Design Alternative (EDA) II, also referred to as the Hot Drift Cool Pillar design [3]. The relevant EDA-II design specifications are presented in Table 1. DOE intends to place the drifts far enough apart so that a significant portion of the pillars may remain below the boiling temperature for water to facilitate infiltrating and thermally driven water above the repository to flow through the cool pillars. The rock in the immediate vicinity of the drifts may be heated above boiling, which may reduce seepage into the drift during the thermal period. Thus, drift spacing, WP spacing, blending of the waste types, and active ventilation before closure are the design criteria to control temperature and limit flow into the drifts.

Table 1. Relevant repository design information [3]

Selected design characteristics	EDA-II
Design basis areal mass loading	60 MTHM/acre
Emplacement area	~1,050 acres
Drift spacing	81 m (center to center)
Drift diameter	5.5 m
Invert	Crushed tuff ballast in and around a steel frame
Number of WPs (based on various waste types)	10,039
Total length of emplacement drifts	54 km
End-to-end distance between WPs in a drift	0.1 m
WP materials	2 cm Alloy 22 (outer overpack) 5 cm Type 316L SS (inner overpack)
Maximum WP capacity	21 pressurized water reactor assemblies
Drip shield	2 cm Ti-Grade 7

Table 1. Relevant repository design information [3] (continued)	
WP heat output at emplacement	20% blending* of spent nuclear fuel assemblies to achieve a maximum thermal output of 11.8 kW per waste package at the time of emplacement (a design consideration)
Designed emplacement backfill	No (natural backfilling could occur)
Preclosure period	50–150 yr
Preclosure ventilation rate (50 yr)	10-15 m^3/s air flow in emplacement drifts
*Blending refers to placing low heat output fuel with high heat output fuel within a waste package.	

WP, drip shield, and invert are the key engineered barriers in EDA-II. The WP design for HLW disposal consists of a large cylinder (i.e., approximately 1.8-m diameter and 5.3-m length) that includes a 20-mm-thick Alloy 22 outer overpack and a 50-mm-thick Type 316L stainless steel (SS) inner overpack in the drift on v-shaped supports. All are emplaced on an invert (i.e., a platform). A drip shield, made of Titanium Grade 7, covers the top and sides of the WP and extends the length of the emplacement drift. The drip shield is intended to protect the WP from dripping on its surface, especially during the thermal reflux period when environmental conditions could be conducive to crevice corrosion. Prior to repository closure, active ventilation of the drifts will control the RH and remove a substantial fraction of the heat emitted by the waste and, thus, keep temperature below the threshold at which cladding failure could occur. Although backfill is not a part of the EDA II design, natural backfilling could occur because of drift collapse.

III. CONCEPTUALIZATIONS OF POTENTIAL REPOSITORY AND GEOLOGIC SETTING

The average rock temperature at the potential repository horizon is calculated using a conduction-only model (i.e., the time history of temperature for each subarea is calculated accounting for the amount of emplaced waste). The WP surface temperature is calculated using a multimode heat transfer (i.e., conduction, convection, and radiation) model based on thermal output from the WP and the repository horizon temperature. Temperature calculations consider (in all cases unless stated otherwise) ventilation during the preclosure period (that could potentially reduce peak WP temperature), no backfill during the postclosure period, and the presence of the drip shield. RH is computed using the standard thermodynamic

equation relating vapor pressure to temperature. Calculations with a hypothetical backfill are shown as a special case.

III.1 Mountain-Scale Heat Transfer

The repository-horizon average rock temperature is computed using an analytic conduction-only model for mountain-scale heat transfer. The model is based on rectangular (strip) thermal sources, representing drifts, separated by the drift spacing and residing in a semi-infinite medium. The modeled repository region has strip sources laid out parallel to each other to cover the potential repository (Figure 1). Each strip source is at a depth of *H* below the ground surface and is represented as a high aspect-ratio rectangular element with a length of 2L and width of 2B (the drift diameter). Because more than one strip source exists, the temperature increase in the semi-infinite medium is the sum of the contributions from each strip source. The general solution for the temperature increase at any point in space and time for a single strip source is given by [4, 5].

$$\Delta T(x,y,z,t) = \int_0^t \frac{\alpha q''_{\text{rep}}(t')}{4k\sqrt{\pi}} \frac{1}{\sqrt{4\alpha(t-t')}} \left[\text{erf}\left(\frac{L-x}{\sqrt{4\alpha(t-t')}}\right) + \text{erf}\left(\frac{L+x}{\sqrt{4\alpha(t-t')}}\right)\right] \left[\text{erf}\left(\frac{B-y}{\sqrt{4\alpha(t-t')}}\right) + \text{erf}\left(\frac{B+y}{\sqrt{4\alpha(t-t')}}\right)\right] \left[\exp\left(\frac{-z^2}{4\alpha(t-t')}\right) - \exp\left(\frac{-(z-2H)^2}{4\alpha(t-t')}\right)\right] dt' \quad (1)$$

where,

$\Delta T(x,y,z,t)$	—	increase in temperature at time *t* at points *x*, *y*, *z* in the semi-infinite medium due to one strip source [°C]
$q''_{\text{rep}}(t)$	—	time-dependent repository heat flux [W/m^2]
α	—	thermal diffusivity of the semi-infinite medium [m^2/s]
k	—	thermal conductivity of the semi-infinite medium [W/(m °C)]

L	—	half-length of a strip source [m]
B	—	half-width of a strip source [m]
H	—	depth of a strip source below the ground surface [m]
t	—	actual time after activation of heat flux [s]
t'	—	time of integration [s]
x,y,z	—	location of interest [m]

A similar formulation was also used in [6]. The integral can be computed using any standard numerical technique. In our application, the Gauss-Legendre quadrature method [7] was used.

For ease of use and computational efficiency, the model replaces the intricate repository layout and the complex geologic setting with relatively simple conceptual representations. The repository layout is represented by an idealized planar feature discretized into a set of subareas. Figure 1 shows a top view of the repository layout. As illustrated in Figure 1, quadrilateral

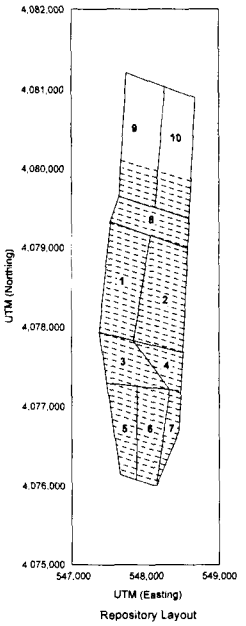

Figure 1. Heat sources represented as parallel dotted lines in the modeled repository region. The figure shows the top view of the repository layout

subareas of uniform thickness are used to represent individual subregions of the potential repository. In the current application, the potential repository is divided into 10 subareas. The number of WPs in each subarea is assumed proportional to the fraction of the total potential repository area represented. The geology above and below the repository is replaced by an equivalent medium (i.e., homogenous) with properties the same as those of the rock in which the drifts are excavated.

The ground surface is assumed exposed to atmospheric conditions with a constant temperature (currently not affected by climate change). The analytic equation is valid below the ground surface, $z < H$. The repository-scale heat flux is related to the areal mass loading (AML) and heat output per metric ton of uranium (MTU) waste:

$$q''_{\text{rep}}(t) = \text{AML}\ Q_{\text{MTU}}(t) \tag{2}$$

Likewise, the thermal output for a single WP is related to the WP payload:

$$Q_{\text{wp}}(t) = \text{MTU}_{\text{wp}}\ Q_{\text{MTU}}(t) \tag{3}$$

where,

AML — areal mass loading for the area occupied by the drifts [MTU/m^2]

MTU_{wp} — metric tons of uranium in a representative WP

$Q_{\text{MTU}}(t)$ — time-dependent heat output per MTU of waste [W/MTU]

The thermal outputs, $Q_{\text{MTU}}(t)$, are based on an average of pressurized water reactor (PWR) and boiling water reactor (BWR) WPs. An average burnup of 37 GWd/MTU is used, which is based on 65-percent PWR waste with a 39.56-GWd/MTU burnup and 35 percent BWR waste with a 32.24-GWd/MTU burnup. Figure 2 represents the thermal output as a function of time for the average waste and the PWR and BWR wastes.

WPs are emplaced in drifts so close to each other that there is essentially no spatial variation in the waste heat output along the drift, however, there is significant variation in heat output between the drifts. Figure 3 shows a plan view of the potential repository with parallel emplacement drifts and periodically spaced WPs.

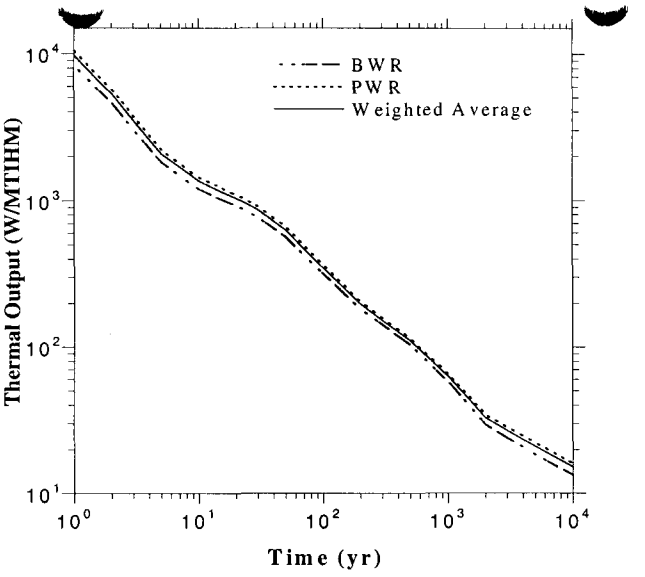

Figure 2. Heat output from an average fuel mix and burnup as a function of time after emplacement. (TIHM – metric tons of initial heavy metal)

Because of the variation in heat losses, the temperature varies significantly between drifts (i.e., between the strip sources). The temperature increase at any point is because of the contribution from all strip sources. For each subarea, the average rock temperature is computed at an elevation half the drift diameter in the drift nearest the center of the subarea. The analytic mountain-scale conduction model predicts the drift temperature, T_{rock} as a function of time. Having computed T_{rock} for the subarea, the WP surface temperature can be calculated.

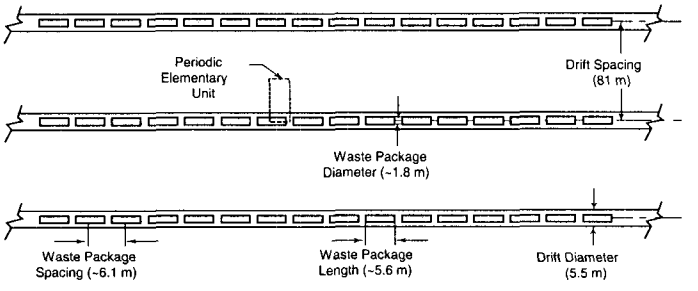

Figure 3. Plan view of potential repository showing emplacement drifts and WPs

III.2 Ventilation

Ventilation during the preclosure period (50–150 years) could impact the temperature field computed by the conduction-only model presented previously. Ventilation is expected to keep the temperature low at the WP surface and drift wall. To account for ventilation, the heat flux from the strip sources is adjusted by the factor for ventilation heat losses, f_v (Table 2):

$$q''_{\text{rep}}(t) = (1 - f_v) q''(t)|_{\text{nv}} \tag{4}$$

where $q''(t)|_{\text{nv}}$ represents no-ventilation thermal output. As shown by Eq. (4) and Table 2, ventilation during the preclosure period is assumed to reduce the heat flux by 70 percent [8]. This assumption is based on DOE's assessment that 70 percent of the heat generated by the waste packages must be removed to keep boiling fronts from coalescing in the rock pillars.

Table 2. Parameters for determining repository scale and drift-scale heat transfer [1]

Parameter	Mean Value
Emplacement drift spacing	81 m
WP spacing along emplacement drift (center-to-center distance)	6.14 m
Total waste emplaced in repository	70,040 MTU
WP payload	7.89 MTU
Number of equivalent WPs (purely on the basis of mass per WP)	8,877
Age of waste	26 yr
Ambient repository temperature	20 °C
Mass density of Yucca Mountain rock	2,580 kg/m^3
Specific heat of Yucca Mountain rock	840 J/(kg-K)
Thermal conductivity of Yucca Mountain rock	1.56 W/(m-°C)
Emissivity of drift wall	0.8
Emissivity of drip shield	0.63
Emissivity of WP	0.87

Table 2. Parameters for determining repository scale and drift-scale heat transfer [1]	
Parameter	**Mean Value**
Thermal conductivity of floor	0.6 W/(m-°C)
Effective thermal conductivity (with natural convection)	0.9 W/(m-°C)
Factor for ventilation heat losses, f_v	0.70
Time of repository closure	50 yr
Effective thermal conductivity of the hypothetical backfill	0.27 W/(m-°C)
Elevation of repository horizon (affects the boiling point of water)	1,072 m
Elevation of ground surface (used in determining the thickness of the rock mass above the repository)	1,400 m
Note: For the probabilistic case, thermal conductivity of Yucca Mountain rock was assigned a triangular distribution: Minimum = 1.34, Most likely = 1.59, Maximum = 1.75 W/(m-°C)	

A multimode (i.e., conduction, convection, and radiation) heat transfer model is used for modeling drift-scale heat transfer. Figure 4 shows the schematic and an idealization of the cross section of a drift with a WP, drip shield, backfill, and invert for computing drift-scale heat transfer. This idealization in which the two-dimensional geometric cross section of the drift is replaced by a radially oriented configuration centered on the drift centerline is assumed acceptable [9, 10]. A simplified thermal network is used to determine the WP surface temperature given T_{rock} (from the mountain-scale model described previously) and $Q_{wp}(t)$.

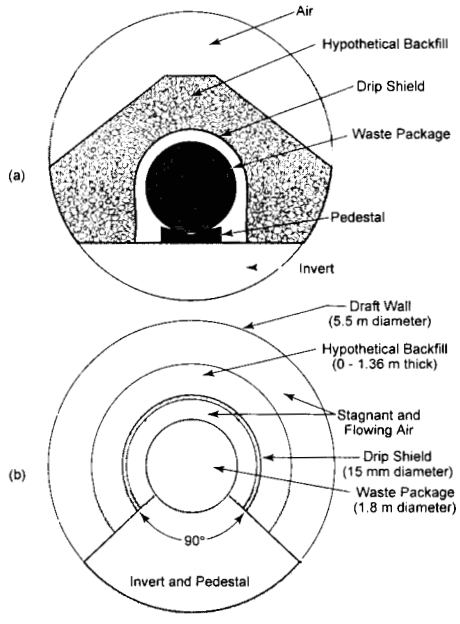

Figure 4. Schematic showing idealization of the emplacement for performing thermal calculations

Equations (5) and (6) are used to solve for WP surface temperature, given the rock temperature, thermal output of the WP, and thermal conductances. Heat is transferred by thermal radiation and natural convection in the backfilled region around a WP and by conduction through the drip shield, backfill (if present), and through the WP support and floor material (e.g., invert) as

$$Q_{\mathrm{wp}} = G_{\mathrm{tot}}\left(T_{\mathrm{wp,surf}} - T_{\mathrm{rock}}\right) \tag{5}$$

$$G_{\mathrm{tot}} = G_{\mathrm{cond|floor}} + \frac{1}{\left[\frac{1}{G_{\mathrm{rad1}} + G_{\mathrm{conv1}}} + \frac{1}{G_{\mathrm{cond|bfds}}} + \frac{1}{G_{\mathrm{rad2}} + G_{\mathrm{conv2}}}\right]} \tag{6}$$

where,

Q_{wp} — time-dependent thermal output for a WP adjusted for ventilation during the preclosure period [W]

G_{tot} — total conductance [W/°C]

G_{rad1}, G_{rad2} — equivalent thermal conductance for radiative heat transfer below the drip shield and above the drip shield, respectively [W/°C]

G_{conv1}, G_{conv2} — equivalent thermal conductance for convective heat transfer below the drip shield and above the drip shield, respectively [W/°C]

$G_{cond|floor}$ — effective thermal conductance for conductive heat transfer through the pedestal/floor [W/°C]

$G_{cond|fbfds}$ — effective thermal conductance for conductive heat transfer through the drip shield and, if present, backfill [W/°C]

T_{rock} — drift wall temperature [°C]

$T_{wp,surf}$ — WP surface temperature [°C]

According to [11], the thermal conductance for radiative heat transfer can be represented via a linearization of the Stefan-Boltzmann law. Thus, the radiative heat transfer above the WP that accounts for the emissivity of the WP and drift rock wall can be represented by

$$G_{\text{rad}} = fc \frac{4\sigma\left(273.15 + T_{\text{rock}}\right)^3}{\frac{1-\varepsilon_i}{\varepsilon_i \pi D_i\left(L_{\text{wp}} + 2\delta\right)} + \frac{1}{F_{i-o}\pi D_i\left(L_{\text{wp}} + 2\delta\right)} + \frac{1-\varepsilon_o}{\varepsilon_o \pi D_o\left(L_{\text{wp}} + 2\delta\right)}} \tag{7}$$

where,

f_c — fraction of the WP surface contributing to heat transfer [unitless]

σ — Stefan-Boltzmann constant [= 5.67 × 10^8 W/(m^2K^4)]

ε_i, ε_o — emissivity of the inner and outer surfaces, respectively [unitless]

D_i, D_o — diameter of the inner and outer surfaces, respectively [m]

L_{wp} — length of the WP [m]

F_{i-o} — radiative view factor from the inner surface to the outer surface (= 1) [unitless]

2δ — gap between WPs along a drift [m]

The subscript *i* represents the WP surface during the preclosure period. During the postclosure period, subscript *i* represents the WP surface and the outer drip shield surface (or the backfill surface, if present) for regions 1 and 2, respectively. The subscript *o* represents the drift wall during the preclosure period. During the postclosure period, subscript *o* represents the inner drip shield surface and the drift wall for regions 1 and 2, respectively.

A fraction of the WP area is available for the radiative/convective heat transfer and the remainder (i.e., the bottom of the package) participates in conduction through the pedestal/floor. Thermal conductances for convective heat transfer above the WP and conductive heat transfer below the WP are computed from

$$G_{\text{conv}} = f_c \frac{2\pi k_{\text{eff,nc}}\left(L_{\text{wp}} + 2\delta\right)}{ln\frac{D_o}{D_i}} \tag{8}$$

$$G_{\text{cond}} = \left(1 - f_c\right)\frac{2\pi k_{\text{floor}}\left(L_{\text{wp}} + 2\delta\right)}{ln\frac{D_{\text{rw}}}{D_{\text{wp}}}} \tag{9}$$

where,

$k_{\text{eff,nc}}$ — effective thermal conductivity representation of natural convection [W/(m -°C)]

k_{floor} — thermal conductivity of the concrete pedestal/floor material [W/(m -°C)]

The effective axial length for conductive and convective transfers from the WP to the drift wall should be larger than the length of the WP. A reasonable value for this length is chosen as the WP spacing (i.e., $L_{\text{wp}} + 2\delta$).

For backfilled drifts, conductive heat transfer through the space above the floor (i.e., invert) can be predicted using an effective thermal conductance for the backfill material

$$G_{\text{cond|bfds}} = f_c \frac{2\pi\left(L_{\text{wp}} + 2\delta\right)}{\frac{1}{k_{\text{eff,bf}}} ln\frac{D_{\text{bfo}}}{D_{\text{dso}}} + \frac{1}{k_{\text{ds}}} ln\frac{D_{\text{dso}}}{D_{\text{dsi}}}} \tag{10}$$

where,

$G_{\text{cond/bfds}}$ — effective thermal conductance if the backfill is present [W/°C]

$k_{eff,bf}$ — effective thermal conductivity of backfill material [W/(m -°C)]

k_{ds} — thermal conductivity of drip shield [W/(m -°C)]

D_{dso} — outer diameter of the drip shield [m]

D_{dsi} — inner diameter of the drip shield [m]

D_{bfo} — equivalent diameter of emplaced backfill [m]

The formalisms presented previously [especially, Eq. (6)] can be extended by using the effective thermal conductivity of materials inside the WP [12] to obtain the temperature inside the WP.

III.3 Relative Humidity

The WP temperature and RH are required input for the drip shield and WP corrosion and radionuclide release calculations in the system model. The RH is defined as the ratio of the actual vapor pressure to the vapor pressure at the WP surface [13]:

$$\mathrm{RH} = \frac{P_{\mathrm{V}}\left[\min\left(T_{\mathrm{b}}, T_{\mathrm{W}}\right)\right]}{P_{\mathrm{V}}\left(T_{\mathrm{wp}}\right)} \tag{11}$$

where,

P_v — vapor pressure as a function of temperature [Pa]

min (T_b, T_w) — minimum of T_b or T_w

T_b — boiling point temperature [~370 K at potential repository]

T_w — drift wall temperature [K]

T_{wp} — WP surface temperature [K]

Below boiling conditions, the definition of RH used in Eq. (11) is equivalent to the mole fraction definition of RH frequently found in thermodynamic textbooks [14, 15]. RH is generally defined as the actual mole fraction of water vapor in the air divided by the maximum or saturation mole fraction of water vapor in the air at the same temperature and pressure. Below boiling conditions, mole fractions are related to the vapor partial

pressures, so, this definition is equivalent to Eq. (11). Vapor pressures (P_{vap}) are computed as a function of temperature using [16]

$$\ln\left(\frac{p_{vap}}{p_c}\right) = \left(v_{pa}\left(1-\frac{T}{T_c}\right) + v_{pb}\left(1-\frac{T}{T_c}\right)^{1.5} + v_{pc}\left(1-\frac{T}{T_c}\right)^{3} + v_{pd}\left(1-\frac{T}{T_c}\right)^{6}\right)\left(\frac{T}{T_c}\right)^{-1} \quad (12)$$

where $v_{pa}, v_{pb}, v_{pc}, v_{pd}$ are reference values (i.e., constants) and p_c and T_c are critical pressure and temperature for water, respectively. Above boiling conditions, the vapor partial pressure is not allowed to exceed the atmospheric pressure (a conservative assumption). When the WP surface temperature exceeds the boiling point, it is preferable to define RH as a ratio of the two vapor pressures specified previously, which is consistent with the technical literature [17-19].

To capture the repository edge heat losses, either more subareas need to be created along the edges or the temperatures can be calculated at the edge (as opposed to the center) of the subareas.

IV. SYSTEM MODEL

At the system level, calculations can be performed both deterministically and probabilistically. The probabilistic approach that accounts for parametric uncertainties provides a range of results that show the combined effects of the inherent variance in the value of a parameter and lack of complete knowledge of the phenomenon. Also, trends not evident in the results from the deterministic data may become evident in the probabilistic results.

Probabilistic sampling is conducted using Latin Hypercube Sampling [20]. Each realization uses a set of values generated from the probability distribution functions specified in the system model. The probability distribution functions are based on available data and also reflect the uncertainty in the parameters. For purposes of this paper, only thermal conductivity of the repository rock is sampled (350 realizations). The rest of the parameters are set at the mean values for various reasons including (i) the parameter is a physical constant, the parameter is set at a conservative value in the absence of sufficient information, or (iii) the prior sensitivity studies have identified that model output is sufficiently insensitive to that parameter. The system model, however, imposes no restrictions on changing these constant parameters to sampled parameters.

Decreasing the number of sampled parameters reduces the number of Monte Carlo realizations needed for various analyses.

V. ASSUMPTIONS

- The semianalytic model presented in this paper simplifies the problem by using uniform rock thermal properties and uniform heat loading at the repository level with drift-size two-dimensional planar sources. Note the mountain-scale calculations can also be performed using WP-size heat sources [i.e., by considering each WP (as opposed to the drift) as a planar heat source]. For computational expediency, calculations are carried out using drift scale heat sources. Waste package scale heat sources can be used to determine the significance on temperature of the waste package-scale variations in thermal outputs.
- The mountain-scale conduction model assumes the ground surface is at a constant temperature and is not affected by climate change.
- The repository has enough ventilation shafts and drifts that a sharp increase in temperature along the drift will not develop in the direction of the ventilation.
- Radiation heat loss from the top of the backfill to the surrounding rock mass is negligible.
- For computational efficiency, the method assumes the temperature at one location can be representative of the entire subarea. To capture the repository edge heat losses, either more subareas need to be created along the edges or the temperatures can be calculated at the edge (as opposed to the center) of the subareas.
- The back-calculation of representative WP temperature from the drift wall temperature assumes the heat transfer in the drift is quasi-steady state.
- Heat dissipation by the WP is based on the assumption of an average WP.
- Quasi-steady-state heat transfer through the hypothetical backfill can be represented by an effective backfill thermal conductivity.
- There is no cold trap effect along the drift that would lead to moisture redistribution or elevated RH at some locations.

- The repository rock mass has a rock well-connected fracture network that facilitates seepage through the rock and maintains pressure in the drift close to atmospheric pressure.
- Eq. (11) for relative humidity assumes that the drift walls are wet with liquid water when the wall temperature is below boiling, and that pure steam is continuously available at the drift wall when the wall temperature is above boiling (e.g., the steam partial pressure is set at 1 atm when the wall temperature is above boiling). This could lead to over estimation of relative humidity.
- The unheated cold ends of the drift will always have lower drift wall temperatures than the heated portion, which could create a vapor concentration gradient that will drive vapor mass transfer from the heated region to the cold ends, drying the heated region. This should be verified via detailed modeling studies.
- Ventilation during the preclosure period is assumed to reduce the heat flux from the strip sources by 70 percent [8].
- The thermal conductivity of the rock mass remains constant over the entire simulation period. This assumption is made on the basis of two factors: (i) the matrix water saturation several meters from the drift wall into the rock mass remains high and does not change substantially [21], and (iii) the temperature effect on thermal conductivity is not significant.

VI. RESULTS

Calculations were performed using the semianalytical model with the system model framework, both deterministically and probabilistically using the parameter mean values and parameter values sampled from distribution functions, respectively. As indicated earlier, only the rock thermal conductivity parameter was sampled. For brevity, results from only the probabilistic calculations are shown unless stated otherwise. The input parameters used to compute temperature and RH are presented in Table 2. All calculations are shown without backfill (i.e., the EDA-II design) unless explicitly stated otherwise. Peak WP temperatures shown in Figures 5, 6, and 8 are similar to those obtained in [22].

The probabilistic calculation is based on 350 Monte Carlo realizations. In each realization, the semianalytic thermal model was invoked 10 times (once for each subarea). Therefore, for a 350-realization probabilistic run, the thermal model was invoked 3,500 times. The thermal calculations presented in the

semianalytic model executed within only a fraction of a second compared with the time required to perform calculations for each realization, which took on the order of 70 seconds. This efficiency with which the semianalytic model executes is important from a run-time standpoint.

Figure 5 shows the average, minimum, and maximum WP temperatures for subarea 1. The sharp rise in temperature at 50 years corresponds to the time of repository closure when ventilation stops. The range between the minimum and maximum temperatures is approximately 20 °C for the time period of 100–1,000 years. Subareas 2–10 exhibit the same general variability in the average, minimum, and maximum WP temperatures as subarea 1. The largest minimum-to-maximum difference within a subarea for all 350 realizations is 25 °C; this difference occurs around 90 years. This one large difference indicates that uncertainty in the thermal conductivity of the rock surrounding the repository has a significant influence on the

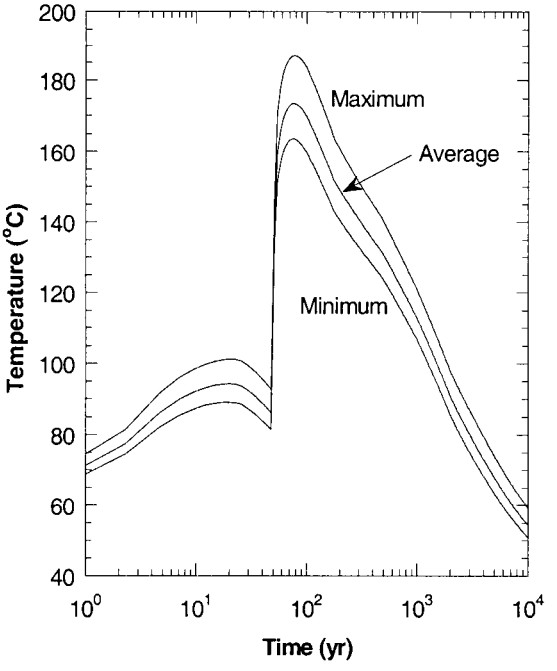

Figure 5. Maximum, minimum, and average WP surface temperatures in subarea 1 from 350 Monte Carlo realizations

range of computed WP temperatures. Although not shown, this uncertainty has a corresponding influence on WP surface RH. This difference could affect the SNF dissolution and corrosion calculations because the corrosion rate is sensitive to the WP temperature, especially if localized corrosion is a possibility.

Figure 6 shows the subarea-to-subarea variability in WP surface temperature. The subarea-to-subarea variability in the WP temperature in the 400- to 10,000-year time period is greater than 10 °C with a maximum temperature difference of 20 °C at 1,600 years. The subarea-to-subarea variability in the WP temperature from 0 to 400 years and from 10,000 to 100,000 years is less than 10 °C. Note the subarea-to-subarea variability in temperature shown here may not be fully reflective of the edge effect (i.e., heat losses at the

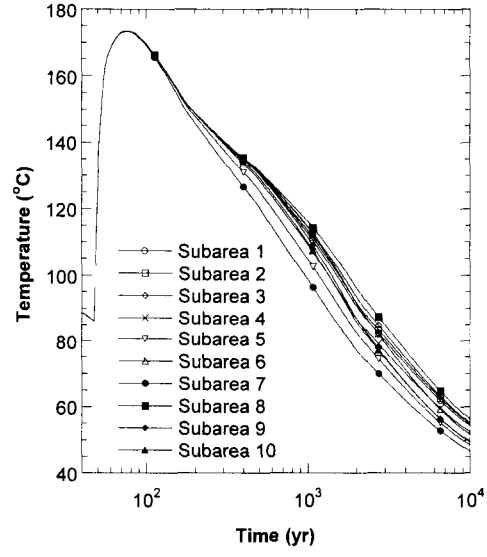

Figure 6. Subarea-by-subarea variation in WP surface temperature (averaged for 350 Monte Carlo realizations for each subarea)

periphery of the subarea—thus, lower Subareas 1 and 2 are the largest, and subarea 7 is the smallest (located away from the center of the repository and having an elongated shape). In the largest two subareas, WPs cool slower compared with the smallest subarea because subarea 7 is affected more from the edge cooling effect than subareas 1 and 2. Cooling is the slowest in subarea 8 because it has less exposed cooling edges and is more centrally located than the other subareas. Because the temperature for a subarea is determined at its center, the distance of this point from the cooling edge strongly influences predicted temperature in a subarea.

Figure 7 shows probabilistic calculations for WP surface RH for each subarea. This figure shows trends that correspond to those from temperature when compared on a subarea-to-subarea basis. Namely, after closure and at earlier times (prior to 2,000 years), subarea 8 shows the lowest RH of any subarea, and subarea 7 shows the highest.

Subarea-dependent temperature and RH values from the near field are used by the WP degradation model to determine WP failure time. Consequently, WP failure time may be different for each subarea. Depending on the selection of the model, SNF dissolution rate is also a function of temperature. Therefore, the SNF dissolution rate and, thus, the quantity of radionuclides available for release, can be different for each subarea.

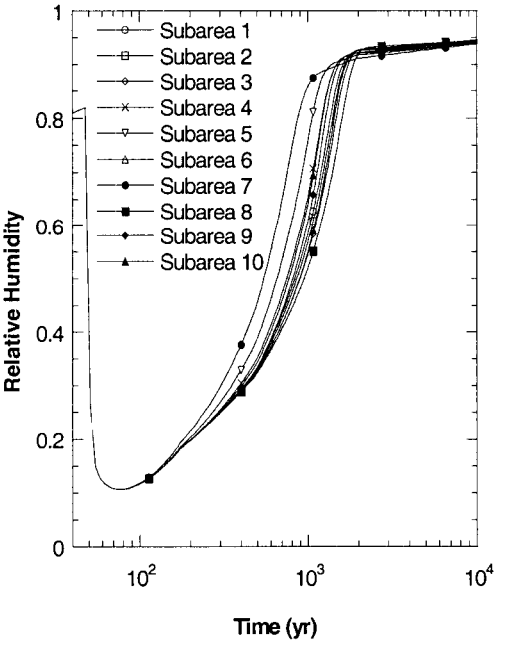

Figure 7: Subarea-to-subarea variation in WP surface RH (averaged for 350 realizations for each subarea.

Figure 8 shows the trend in WP temperature evolution as a function of the thickness of a hypothetical backfill in between the drip shield and the drift wall. The maximum thickness of the hypothetical backfill is 1.36 m (the radial distance between the outer wall of the drip shield and the drift wall). The figure shows temperature behavior as a function of the percentage backfilled (constant throughout the postclosure period) for subarea 1 with other parameters set to their mean values. For the 100 percent backfill case, a peak

temperature of 353 °C occurs at 54.5 years. By comparison, the estimated peak WP temperature without backfill occurs at 77.3 years and is 173 °C. These values are dependent on the heat transfer modes and associated model parameters, which require further investigation.

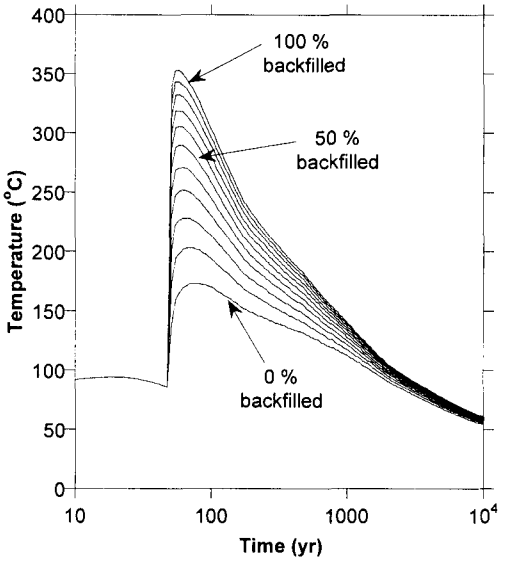

Figure 8. WP temperature in subarea 1 as a function of thickness of a hypothetical backfill for the mean value data set

VII. CONCLUSIONS

This paper presents an abstracted model for estimating temperatures in a probabilistic model that requires thousands of Monte Carlo realizations to compute the performance of the repository system and determine influential models and parameters. The model estimates the repository-horizon rock temperature using a mountain-scale analytic heat conduction model with drifts represented as heat sources. To estimate the WP surface temperature from the rock temperature, a thermal network model represents the details of the drift (the drip shield, invert, various air gaps in between, and potential backfill) and various heat transfer models (i.e., conduction, convection, and radiation). Vapor pressure is computed using the standard thermodynamic equation relating vapor pressure to temperature.

Results indicate that the temperature near the center of the potential repository is nearly 165 °C on an average, and the temperature shows sensitivity to the presence or absence of a hypothetical backfill. In

addition, the WP temperature remains above boiling for nearly 1,000 years even without the hypothetical backfill. The trend in RH is closely related to the trend in the temperature difference between the WP surface and the drift wall.

The presence of a hypothetical backfill results in an increasing trend in temperature, with the peak WP temperature for the fully backfilled condition approximately double that for the no-backfill condition under the assumption made about the backfill thermal characteristics. Also, with backfill, the time span for which the estimated temperature remains above boiling is much longer than in the no-backfill case.

In the future, results from the semianalytical model presented in this paper (which approximates mountain-scale heat transfer to be conduction only) may be compared against a detailed numerical simulation of a coupled thermohydrology process. The cold-trap effect will be incorporated in the abstracted model if detailed calculations will show that it has significant influence on relative humidity along the drifts, which could impact WP life adversely.

VIII. ACKNOWLEDGMENTS

We thank Randy Fedors and Steve Green for their helpful technical reviews. We also acknowledge the involvement of R. Manteufel during the early stage of model development, which shaped the framework of the model. The paper was prepared to document work performed by the Center for Nuclear Waste Regulatory Analyses (CNWRA) for the U.S. Nuclear Regulatory Commission (NRC) under Contract No. NRC–02–02–012. The activities reported here were performed on behalf of the NRC Office of Nuclear Material Safety and Safeguards, Division of High-level Waste Repository Safety. The paper is an independent product of CNWRA and does not necessarily reflect the views or regulatory position of NRC.

IX. REFERENCES

[1] Mohanty, S., J. McCartin, and D. Esh. (coordinators) *Total-system Performance Assessment (TPA) Version 4.0 Code: Module Description and User's Guide*. San Antonio, TX: Center for Nuclear Waste Regulatory Analyses. 2002.

[2] Mohanty, S., G.A. Cragnolino, T. Ahn, D.S. Dunn, P.C. Lichtner, R.D. Manteufel, and N. Sridhar. *Engineered Barrier System Performance Assessment Code: EBSPAC Version 1.1 Technical Description and User's Manual.* CNWRA 97-006. San Antonio, TX: Center for Nuclear Waste Regulatory Analyses. 1997.

[3] Civilian Radioactive Waste Management System, Management and Operating Contractor. *License Application Design Selection Report.* B00000000–01717–4600–00123. Revision 01. Las Vegas, NV: Civilian Radioactive Waste Management System, Management and Operating Contractor. 1999.

[4] Claesson, J. and T. Proberts. *Temperature Field Due to Time-Dependent Heat Sources in a Large Rectangular Grid—Derivation of Analytical Solution.* SKB 96-12. Stockholm, Sweden: Swedish Nuclear Fuel and Waste Management Co. 1996.

[5] Carslaw, H.S. and J.C. Jaeger. *Conduction of Heat in Solids.* London, United Kingdom: Oxford University Press. 1959.

[6] U.S. Department of Energy. *Viability Assessment of a Repository at Yucca Mountain. Overview* and all five volumes. DOE/RW–0508. Las Vegas, NV: U.S. Department of Energy, Office of Civilian Radioactive Waste Management. 1998.

[7] Press, W.H., S.A. Tekolsky, and W.T. Vetterling and B.P. Flannery. *Numerical Recipes in FORTRAN.* Cambridge, United Kingdom: Cambridge University Press. 1992.

[8] CRWMS M&O. "Ventilation Mode." ANL–EBS–MD–000030. Revision 00. Las Vegas, Nevada: CRWMS M&O. 1999.

[9] Fedors, R.W., S. Green, D. Walter, G. Adams, D. Farrell, and S. Suedaman. "Temperature and Relative Humidity along Heated Drifts with and without Drift Degradation." San Antonio, Texas: Center for Nuclear Waste Regulatory Analyses. 2004.

[10] Manepally, C., R. Fedors, G. Adams, and S. Green. "Effects of Drift Degradation on Environmental Conditions in Drifts." Fall Meeting Supplement, American Geophysical Union 2003 Fall Meeting, San Francisco, California, December 8-12, 2003. EOS Transactions, American Geophysical Union. Vol. 84, No. 46. 2003.

[11] Incropera, F.P. and D.P. DeWitt. *Fundamentals of Heat and Mass Transfer*. 3rd Edition. New York: John Wiley and Sons. 1995.

[12] Manteufel, R.D. and N.E. Todreas. Effective thermal conductivity and edge conductance model for a spent fuel assembly. *Nuclear Technology* 105(3): 421–440. 1994.

[13] Manteufel, R.D. Effects of ventilation and backfill on mined waste disposal facility. *Nuclear Engineering and Design* 172: 205–219. 1997.

[14] Van Wylen, G.J. and R.E. Sonntag. *Fundamentals of Classical Thermodynamics*. New York: John Wiley and Sons. 1978.

[15] Moran, J.J. and H.N. Shapiro. *Fundamentals of Engineering Thermodynamics*. New York: John Wiley and Sons. 1992.

[16] Reid, R.C., J.M. Prausnitz, and B.E. Poling. The Properties of Gases and Liquids. Fourth Edition. New York: McGraw-Hill Book Company. 1987.

[17] Hartman, H.L. *Mine Ventilation and Air Conditioning*. Malabar, FL: Krieger Publishing Company. 1991.

[18] Bejan, A. *Advanced Engineering Thermodynamics*. New York: John Wiley and Sons. 1988.

[19] Fyfe, D. *Corrosion*. R.A. Jarman and G.T. Burstein, eds. Oxford, United Kingdom: Butterworth Heinmann. 1: 2:31–2:42. 1994.

[20] Iman, R.L. and M.J. Shortencarier. *A FORTRAN 77 Program and User's Guide for the Generation of Latin Hypercube and Random Samples for Use with Computer Models*. NUREG/CR–3624. Washington, DC: U.S. Nuclear Regulatory Commission. 1984.

[21] Bechtel SAIC Company, LLC. "Drift-Scale Coupled Processes (DST and TH Seepage) Models", MDL-NBS-HS 000015 REV 01, Sept. 2004.

[22] Fedors, R.W., G.R. Adams, C. Manepally, and S.T. Green. "Thermal Conductivity, Edge Cooling, and Drift Degradation—Abstracted Model Sensitivity Analyses for Yucca Mountain." San Antonio, Texas: Center for Nuclear Waste Regulatory Analyses. 2003.

Table 3. Nomenclature

Parameter	Description
$\Delta T(x,y,z,t)$	Increase in temperature at time t at points x, y, z in the semi-infinite medium due to one strip source [°C]
$q''_{rep}(t)$	Time-dependent repository heat flux [W/m^2]
α	Thermal diffusivity of the semi-infinite medium [m^2/s]
k	Thermal conductivity of the semi-infinite medium [W/(m °C)]
L	Half-length of a strip source [m]
B	Half-width of a strip source [m]
H	Depth of a strip source below the ground surface [m]
t	Actual time after activation of heat flux [s]
t'	Time of integration [s]
x,y,z	Location of interest [m]
AML	Areal mass loading for the area occupied by the drifts [MTU/m^2]
MTU_{wp}	Metric tons of uranium in a representative WP
$Q_{MTU}(t)$	Time-dependent heat output per MTU of waste [W/MTU]
$q''(t)\|_{nv}$	Represents no-ventilation thermal output
Q_{wp}	Time-dependent thermal output for a WP adjusted for ventilation during the preclosure period [W]
G_{tot}	Total conductance [W/°C]
G_{rad1}, G_{rad2}	Equivalent thermal conductance for radiative heat transfer below the drip shield and above the drip shield, respectively [W/°C]

Table 3. Nomenclature (continued)

Parameter	Description
G_{conv1},	Equivalent thermal conductance for convective heat transfer below the drip shield and above

G_{conv2}	the drip shield, respectively [W/°C]
$G_{cond\|floor}$	Effective thermal conductance for conductive heat transfer through the pedestal/floor [W/°C]
$G_{cond\|fbfds}$	Effective thermal conductance for conductive heat transfer through the drip shield and, if present, backfill [W/°C]
T_{rock}	Drift wall temperature [°C]
$T_{wp,surf}$	WP surface temperature [°C]
f_c	Fraction of the WP surface contributing to heat transfer [unitless]
σ	Stefan-Boltzmann constant [= 5.67×10^{8} W/(m^{2}K^4)]
ε_i, ε_o	Emissivity of the inner and outer surfaces, respectively [unitless]
D_i, D_o	Diameter of the inner and outer surfaces, respectively [m]
L_{wp}	Length of the WP [m]
F_{i-o}	Radiative view factor from the inner surface to the outer surface (= 1) [unitless]
2δ	Gap between WPs along a drift [m]
$k_{eff,nc}$	Effective thermal conductivity representation of natural convection [W/(m -°C)]
k_{floor}	Thermal conductivity of the concrete pedestal/floor material [W/(m -°C)]
$G_{cond/bfds}$	Effective thermal conductance if the backfill is present [W/°C]
$k_{eff,bf}$	Effective thermal conductivity of backfill material [W/(m -°C)]
k_{ds}	Thermal conductivity of drip shield [W/(m -°C)]
D_{dso}	Outer diameter of the drip shield [m]
D_{dsi}	Inner diameter of the drip shield [m]
D_{bfo}	Equivalent diameter of emplaced backfill[m]
P_v	Vapor pressure as a function of temperature [Pa]
min (T_b, T_w)	Minimum of T_b or T_w
T_b	Boiling point temperature [~370 K at potential repository]
T_w	Drift wall temperature [K]
T_{wp}	WP surface temperature [K]